Journal of Radiological Protection

Official journal of the Society for Radiological Protection

PAPER

On the use of retrospective dosimetry to assist in the radiological triage of mass casualties exposed to ionising radiation

IOP Publishing | Society for Radiological Protection Journal of Radiological Protection
J. Radiol. Prot. **40** (2020) 1286–1298 (13pp) https://doi.org/10.1088/1361-6498/abc181

On the use of retrospective dosimetry to assist in the radiological triage of mass casualties exposed to ionising radiation

Carlos Rojas-Palma[1], Clemens Woda[2], Michael Discher[3] and Friedrich Steinhäusler[4]

[1] Environment, Health and Safety Institute, Belgian Nuclear Research Center SCK CEN, Mol, Belgium
[2] Institute of Radiation Medicine, Helmholtz Zentrum München, Neuherberg, Germany
[3] Department of Geography and Geology, Paris-Lodron-University of Salzburg, Salzburg, Austria
[4] Department Chemistry and Physics of Materials, Paris-Lodron-University of Salzburg, Salzburg, Austria

E-mail: carlos.rojas.palma@sckcen.be

Received 25 June 2020; revised 9 October 2020
Accepted for publication 15 October 2020
Published 11 November 2020

Abstract

The reconstruction of the Cochabamba (Bolivia) radiological incident (IAEA—International Atomic Energy Agency 2004 The Radiological Accident in Cochabamba STI/PUB/1199 (Vienna: IAEA)) was used to assess and evaluate retrospective dosimetry methodologies. For this purpose an unshielded radioactive source was placed inside a transportation vehicle (bus) resembling a radiological exposure device. External doses were assessed using water and anthropomorphic phantoms that were placed at various positions in the vehicle and equipped with both fortuitous dosimeters (chip cards, mobile phones), individual dosimeters (electronic dosimeters, thermoluminescent and optically stimulated luminescence dosimeters) and in three cases also with blood sample tubes in thermos flasks for cytogenetic methods. This paper gives a detailed description of the experimental setup, the results of the reference dosimetry, including organ dose assessment for the phantom closest to the source, and includes a compilation of the main results obtained by the retrospective dosimetry techniques. Comparison is made to the results of dose reconstruction obtained by IAEA during the response to the Cochabamba incident in 2002.

Keywords: retrospective dosimetry, radiological triage, mass casualties, radiological incidents

(Some figures may appear in colour only in the online journal)

1361-6498/20/+13$33.00 Printed in the UK

1. Introduction

Under ideal circumstances radioactive sources that are daily used in industry and for medical applications have a sealed fate, which is that they are secured and safe from the cradle to the grave. In other words, their whereabouts is registered and the sources are properly disposed of when no longer needed; however, this is not always the case and high strength radioactive sources are either lost, stolen or simply abandoned. That is how a couple of metal scavengers removed a Cs-137 source left behind in an abandoned clinic in the Brazilian city of Goiânia (IAEA 1988), causing to the date one of the largest public exposures to ionising radiation in history. A similar case involving a Co-60 source was registered in India (Pandey 2016) when five people became very ill after being in contact with a 'shining object' in a scrap shop. The shining object was part of medical equipment that had been dumped days before. Although these exposures to ionising radiation have been mainly due to ignorance and motivated by the will to make easy money, there are also cases in which people have advertently used radioactive sources for criminal purposes, such as the case in 2002 (IAEA 2002) when a Chinese industrial decided to harm a business rival by placing an Ir-192 source in the ceiling of the victim's office. In this case not only the victim showed signs of acute exposure to ionising radiation but also 74 other staff members.

In case of a major release of radioactivity into the environment such as in 2011 in Fukushima, World Nuclear Association (2020), the inadvertent spread of contamination by metal scavengers, a criminal or terrorist act that affect a large number of people by exposing them to ionising radiation, there is an imperative need to determine the actual size of the exposed cohort that would require specialised medical care, and separate them from those who need reassurance and from the worried-well.

Moreover, terrorist attacks using radioactive material can in certain circumstances result in a mass casualty scenario. The attack will likely have an international scale and radiation exposure can range from very low to life-threatening. For triage, the demands on capacity in a mass casualty scenario are likely to surpass the possibility of any single laboratory, making trans-national networking essential. Establishment of a sustainable network in biological and physical retrospective dosimetry, as has recently been realised in the European RENEB network (Kulka *et al* 2017), requires regular inter-comparisons as a demonstration of the network's ability to produce consistent results (Wojcik *et al* 2017). Similar activities in biological dosimetry have been carried out in Europe within NATO exercises (Rothkamm *et al* 2013) and MULTIBIODOSE (Jaworska *et al* 2015). Depending on the irradiation scenarios at hand, different biodosimetry methods are available from well-established cytogenetic assays (Depuydt *et al* 2017, Oestreicher *et al* 2017) to new emerging techniques, especially gene expression (Badie *et al* 2013).

In the framework of the European Commission co-funded security research project CATO (CBRN crisis management, architectures, technologies and operational procedures) a group of scientists have been working on a novel technique to perform a quick estimate of the degree of exposure to ionising radiation by examining the radiation fingerprint left in the personal items carried by people on a daily basis, the so-called fortuitous dosimeters and which consist of resistors and display glasses of mobile phones (Inrig *et al* 2008, Fiedler and Woda 2011, Ekendahl and Judas 2012, Discher and Woda 2013, Lee *et al* 2017), chips on debit, identity or credit cards (Woda and Spöttl 2009, Cauwels *et al* 2010, Pascu *et al* 2013), silicates collected from personal objects (Bortolin *et al* 2011, Ademola *et al* 2017), dental ceramics (Ekendahl *et al* 2013), salt (Ekendahl *et al* 2016) and other commonplace materials (Sholom and Mckeever 2014). This technique is known as retrospective dosimetry and has been widely explored

under laboratory conditions by many researchers (Bassinet *et al* 2014). Some overviews have been published (Woda *et al* 2009, Pradhan *et al* 2014, Bailiff *et al* 2016, ICRU, 2019). The innovation and contribution to extending the state-of-the-art of this work lays in the fact that for the very first time the potential of retrospective dosimetry as a viable tool has been assessed and evaluated outside the laboratory and under real conditions. In addition, this technique has been benchmarked against electronic personal dosimeters (EPDs) and reference dosimeters in the personal objects and a comparison against standardised cytogenetic assays has been made. The assessment and evaluation of the proposed technique was carried out during a series of exposures during the reconstruction of the conditions following the irradiation of 55 people when a defect Ir-192 source used to perform gamma-radiography on gas pipe welding in the Bolivian highlands was transported unshielded in the cargo compartment of a bus for an 8 h trip: The Cochabamba incident (IAEA 2004). The following sections in this paper elaborate on the technical setup, reference dosimetry, overview of the main findings and benchmarking work and conclusions.

2. Experimental setup of the field experiment

The experiments reported on in this paper were conducted in a military and therefore secure venue, namely the Schwarzenbergkaserne, which is a facility belonging to the Austrian army. During one week, from 02 to 05 June 2014, two Ir-192 sources of 0.65 and 1.5 TBq were alternatively placed in the baggage compartment of a bus. The weaker source had the same activity as the source of the Cochabamba incident and was used here for comparison with the results of the dose reconstruction experiment carried out by the IAEA in 2004 (IAEA 2004), using the same exposure time of eight hours. The stronger source was used for an inter-comparison (see section 3.4), to have sufficiently high doses within the maximum allowed exposure time (8 h), which would not have been achievable with the weaker source. Both sources were used to perform a series of irradiations of water-filled canisters and both male and female anthropomorphic phantoms of Rando (Alderson Research Laboratories, USA), equipped with personal objects and dosimeters, as depicted in the figures 1–3. For the water canisters closer to the source, personal dosimeters were put in four positions: on the front at the top, on the front at the bottom, left and right. For comparability, two thermoluminescent detectors (TLDs), provided by SCK CEN (LiF:Mg, Cu, P (MCP-N)) and IAEA (LiF:Mg) and one optically stimulated luminescence dosimeters (OSLD) (BeO), provided by the dosimetry service of the Helmholtz Zentrum München (HMGU, now Mirion Technologies Inc.) were used at each position. For the phantoms, TLDS and OSLDs were positioned at three levels: chest, stomach and bottom. Phones and chip cards were attached on the front lower level of each water canister.

As mentioned in the introduction, laboratory inter-comparisons are an important activity for retrospective dosimetry networks. This issue was considered in the present field test by using the experimental setup as a unique opportunity to conduct a laboratory inter-comparison through the EURADOS network (www.eurados.org), bringing together for the first time physical and biological dosimetry in the same (realistic) setup. Five European biodosimetry laboratories participated, four applying the dicentrics assay and one the micronucleus assay. For physical retrospective dosimetry using OSL of resistor substrates, the same 12 laboratories (11 European and one from the US) as in the first inter-comparison, using the same method but in controlled laboratory conditions, participated (Bassinet *et al* 2014). Emphasis was put on the 'full-mode' protocol, with as many extracted resistor components as possible, to maximise sensitivity but participants were also invited to apply the 'fast-mode' protocol, if feasible

Figure 1. Setup of the field experiment: The Ir-192 source is placed in the baggage compartment of the bus, similar as it was the case during the Cochabamba incident (top). Location of the sources inside the baggage compartment of the bus. The end tips of the guidance tubes of both Ir-192 sources (0.65 and 1.5 TBq) were simultaneously fixed on a tripod to ensure similar exposure conditions, regardless of which source was currently being used during the experiment (bottom). The end tips were closer to the seating floor than in the IAEA reconstruction of the Cochabamba incident, in order to maximise the dose to the fortuitous dosimeters.

(see Bassinet *et al* (2014) for details on the measurement protocols). For this purpose, mobile phones were affixed to the anthropomorphic phantoms placed at three positions in the bus: closest to the source and on the next two rows of seats. Blood sample tubes were stored in thermos flasks, kept at body temperature, and fixed to the side of the three phantoms. Reference dose values for each assay were provided by LUXEL® dosimeters in the phones and by BeO dosimeters on the blood sample tubes and thermos flasks.

For the mobile phones on the water canisters, LUXEL® dosimeters were also put inside as well as annealed pieces of display glass attached to the screen as reference doses for the display glass. Chip cards were equipped with a combination of LUXEL® and BeO dosimeters.

The position of the radiation source with dimensions is shown in figure 4. Additionally the positions of the water containers or anthropomorphic phantoms are plotted in the seating configuration of the bus (blue and pink positions, respectively). The phantoms were placed on seat positions P21, P22, P26 and P30. At position P22, the position presumably closest to the source, the phantom was filled with TLDs (including dosimeters on the surface) to assess organ doses, the dose gradient along the height of the torso and the effective dose. Phantom on position 21 was additionally equipped with salt dosimeters at three positions on the surface and dental ceramics in the positions of teeth inside the phantom.

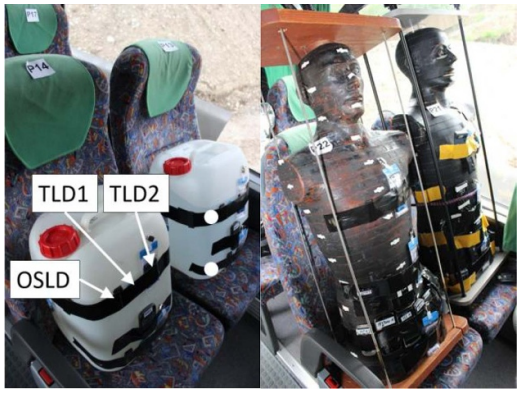

Figure 2. Water-filled canisters with attached mobile phones, chips and personal dosimeters (TLDs, OSLDs) placed on the passengers' seats (left). 'TLD1' refers to the TLD from SCK CEN, 'TLD2' to the TLD from IAEA. The two white circles mark the "front" and 'bottom' positions of the dosimeters, used in figure 6. In addition to the water canisters, four anthropomorphic phantoms equipped with personal and emergency dosimeters were used, one of them filled with TLDs to estimate organ doses and effective dose using conventional methods (right).

Figure 3. Within the framework of an inter-comparison blood sample tubes were put in thermos flasks for keeping the tubes at body temperature and placed at three selected seating positions for subsequent dose estimation using conventional cytogenetic analysis. Selected position of the OSLDs and TLDs on one of the phantom are again marked.

On several rows both seats were equipped with water canisters to investigate scattering and shielding effects. Additional water canisters were positioned along the origin axis of the source to determine rapid decrease of the absorbed dose with increasing distance from the source as expected by the inverse square law.

During the whole experiment a total of 105 samples were irradiated and the main results are reported below.

2.1. Fundamentals of retrospective dosimetry

Following Ainsbury *et al* (2011) retrospective dosimetry can be defined, within the context of physical and biological retrospective dosimetry techniques for individual external exposures, simply as:

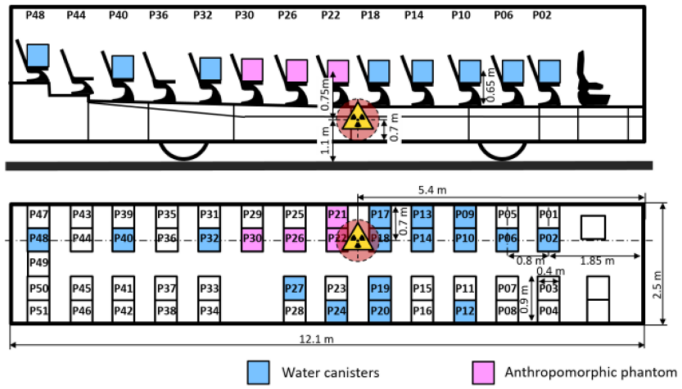

Figure 4. Schematic view of the bus with positions of water canisters (in blue), anthropomorphic phantoms (in pink) and source.

'The estimation of a radiation dose received by an individual recently (within the last few weeks), historically (in the past) or chronically (over many years)'. Such dosimetry methods are usually implemented when conventional 'prospective' dose estimation systems, such as film badge dosimetry are not available or require independent verification or when accidents involve the general public, which generally does not wear official individual dosimeters.

The personal items investigated in this study were analysed using luminescence dosimetry: Ionising radiation absorbed by an insulator or a semiconductor produces free charge carriers that can be trapped at lattice defects of the material. Luminescence dosimetry is based on the stimulated emission of light from these materials by release of the trapped charge carriers and subsequent recombination. Stimulation is performed either thermally (thermoluminescence, TL) or optically (optically stimulated luminescence, OSL). In both cases the amount of emitted and detected light is proportional to the amount of trapped charge carriers and thus proportional to the absorbed dose in the material. Further details of physical and biological retrospective dosimetry techniques can be found in Ainsbury *et al* (2011) and Fattibene and Wojcik (2009).

3. Conduction of the field tests and compilation of main results

3.1. Personal dosimeter readings

In this section the results of the personal dosimeters on the canister/phantoms are compared and discussed. The dosimeter readings serve to map the dose distribution throughout the bus and as a comparison to the doses measured in the personal items and to the Monte-Carlo simulations of the exposure scenario.

In figure 5 the overall comparison between the personal dose equivalents (Hp(10)) as measured by the three different types of personal dosimeters (TLDs from SCK CEN and IAEA, OSLDs from HMGU) for all seats and all positions on the canisters/phantoms is shown. These data were obtained on the second day of exposure using the stronger Ir-192 source (1.5 TBq). The scatter between the different dosimeters is attributable to the sensitivity of the absorbed dose on the exact position of the dosimeter on the canister/phantom, leading to differences in the distance to the source and degree of shielding. Overall a good correlation between the three personal dosimeter systems can be seen, with however some systematic differences from the first expected one to one correspondence. The difference in slopes in figure 5 is possibly due

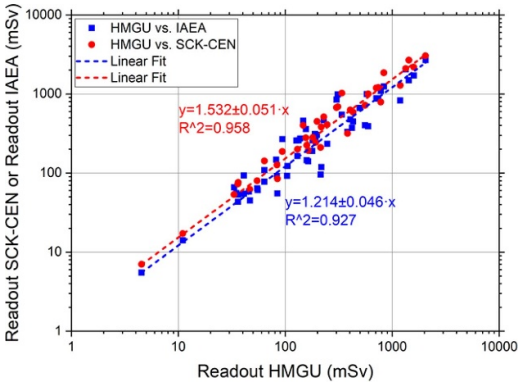

Figure 5. Comparison of the individual dosimeter readings from SCK CEN, IAEA (both TLDs) and HMGU (OSLDs). The blue dashed line marks the linear regression of SCK CEN vs. HMGU dose data, the red dashed line the regression of IAEA vs. HMGU data.

to differences in calibration and energy dependency of the three different types of dosimeters used.

On average, Hp(10) values monitored by the TLDs from SCK CEN are 50% higher than the Hp(10) values measured by the OSLDs from HMGU and 21% higher than the Hp(10) values measured by the TLDs from IAEA (the latter correlation is not shown for the sake of clarity). The data from IAEA on the other hand are on average 21% higher than the data from HMGU. This difference is most likely due to differences in calibration. As personal dosimeters are allowed to have a variation in energy response of $\pm$40% around unity, as different materials are used for the dosimeters here (BeO and LiF) with different energy responses and angular dependences and as different choices are made for at which energy to set the 100% detector response, the observed differences are realistically possible and not an indication that one system gave fundamentally wrong answers. The comparison between the three different types of personal dosimeters thus also serves to visualise the achievable degree of accuracy (20%–30%), even with these kinds of dedicated, engineered materials.

The dose mapping throughout the bus as recorded by the personal dosimeters is shown in figure 6. For the sake of clarity, only the OSLD results are shown here, which also is the largest dataset of the three personal dosimeters used, for both exposure days. For the seats immediately in front (seats 17 and 18) and behind the source (seats 21 and 22) the highest doses are recorded and also the highly heterogeneous nature of the exposure impressively resolved. Highest doses occur for the right 'arm' position on seat 17, the left 'arm' position on seat 18 and the 'bottom' positions on the phantoms on seats 21 and 22. Dose gradients of more than a factor of three along the height of the torso of the phantoms and of more than a factor of ten along the 'shoulder' axis of the water canisters (17 and 18) are evident. This dose heterogeneity is also present for the following seats (13/14 and 9/10) but with decreasing magnitude, as expected. For the opposite seating rows, the shielding of canister on seat 20 by the canister on seat 19 can be seen and doses generally decrease in the direction 'left arm' to 'right arm' position, as it should be. Finally, exposures become more or less homogeneous for seating positions 32 and higher.

For the exposure with the weaker source, a similar map of doses is obtained but scaled down by the lower activity of the source. Interesting here is the difference in dose in the back of canister/phantom to dose in front of the same canister/phantom, which increases or decreases,

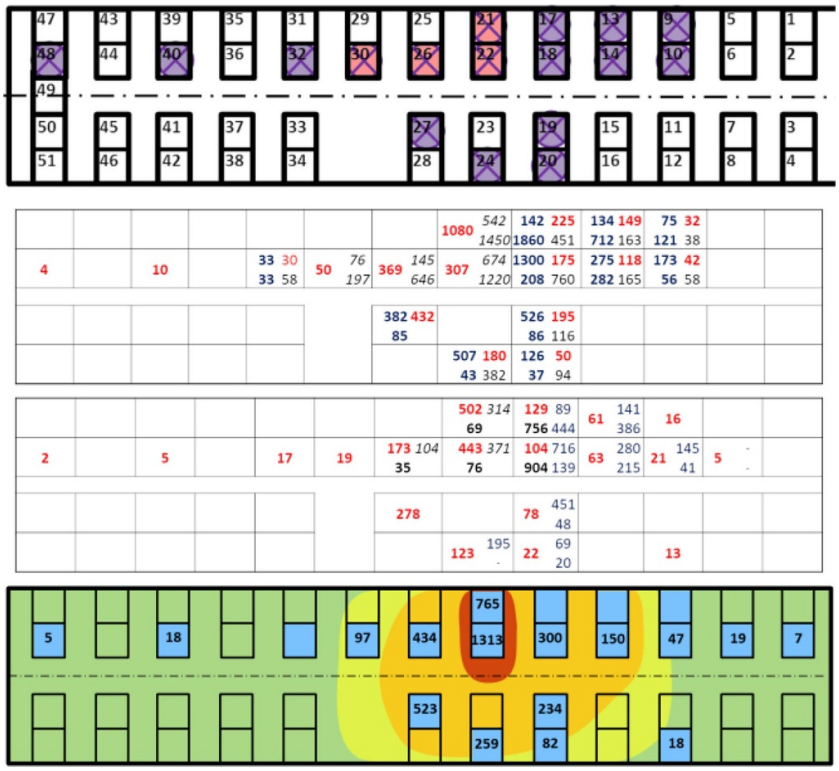

Figure 6. From top to bottom: (1) Seating plan of the bus with marked positions of canisters/phantoms; (2) Results of the OSLD readings for the exposure day with the 1.5 TBq source. Numbers in red: OSLDs attached to the front of the canisters/to the stomach of the phantoms; numbers in blue: OSLDs attached to the left (top row) and right (bottom row) of the canisters; numbers in black: OSLDs attached to the bottom of the canisters; numbers in italics: OSLDs attached to the chest (top row) and bottom (bottom row) of the phantoms; (3) Results of the OSLD readings for the exposure day with the 0.65 TBq source. Numbers in red: OSLDs attached to the front of the canisters/to the stomach of the phantoms; numbers in blue: OSLDs attached left/right; numbers in black (bold): OSLDs attached to the back of the canisters/phantoms; numbers in italics: OSLDs attached to the chest of the phantoms; (4) Results of the EPD readings for the exposure day with the 1.5 TBq source.

depending on seating row, by a factor between 7 and 10 (seats 21/22 and 17/18). The doses reconstructed here are in a similar range but overall somewhat higher than the doses reconstructed by the IAEA in a similar bus experiment following the Cochabamba incident (IAEA 2004). In the latter, the highest dose measured for the base of the water bottle on the seat above the source was 0.5 Gy, in the present setup the highest doses were 0.7–0.9 Gy for the 'left arm' and 'back' positions on the water canisters in front of the source (seat no. 17 and 18). Next to differences in the type of bus and seating configurations used, the main reason is likely the fact that in the IAEA reconstruction, the end of the guide tube was positioned in the middle of the cargo storage compartment, 1.15 m below the seat, whereas in the present experiment, the guide tube was positioned closer to the seating floor (see also figure 1). This was done in order to maximise the dose to the personal items, since they are less radiation sensitive than individual dosimeters.

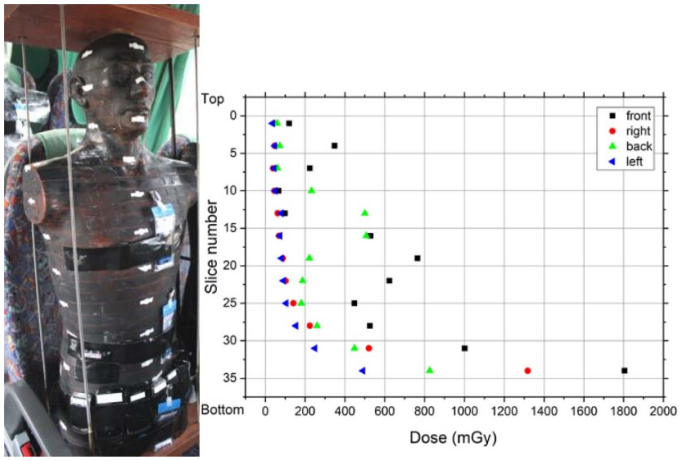

Figure 7. Left panel: Phantom and dosimeters set-up on seat 22. TLD were affixed on the left, right, back and front surface of every fourth slice of the phantom (see white stripes on the phantom). Right panel: Results of the dose gradient on the lateral, front and back surfaces of the phantom.

3.2. Organ dose and effective dose

In the right panel of figure 7, the dose gradients measured on the lateral, front and back surfaces of the male phantom positioned on the closest seat to the source (seat 22) are shown; MCP-N TLDs (LiF:Mg,Cu,P) were positioned on the phantom every four slices (about 7.5 cm), as shown in the left panel of figure 7. These data were obtained on the second day of exposure with the strongest source (1.5 TBq).

The two dose profiles at the left and right lateral phantom surface show a smooth, continuous increase in dose with decreasing distance of the measurement points to the bottom of the phantom; dosimeters on the front and back show more variation in dose values. The observation that the pattern of the doses on the front, next to a general increase with increasing slice number, seems to be similar to the surface anatomy of the phantom implies that self-shielding effects could play a role. Similarly, varying dimensions of the torso slices could lead to varying degrees of attenuation for the dosimeters on the back. For a more quantitative analysis and proof of this assumption, Monte Carlo simulations would be necessary, which were beyond the scope of this paper. It is interesting to note that the inversion of the dose profile with increasing slice number for slices 16 and 19, encompassing the TLDs/OSLDs at 'chest' position and for slices 25 and 28, encompassing the TLDs/OSLDs at 'bottom' position is in full concordance with the readings of the respective individual dosimeters.

The equivalent organ doses in the phantom were measured with MCP-N TLDs calibrated in air and converted to dose in ICRU 40 tissue or bone, the results are listed in table 1. As expected from the dose profiles measured on the phantom surface, a strong dose gradient is observed in the organ doses. The organs situated in the pelvic region or in the lower abdomen region, such as the gonads, the bladder or the prostate, were more exposed and received more dose; the organs in the chest region, such as the lungs, or in the head and neck region, such as the brain, the oesophagus or the thyroid, received considerably less dose. The effective dose was calculated according to ICRP (2007), as 329 mSv with an uncertainty of 22% (2σ). It is clear that for this kind of highly non-homogeneous exposure conditions, with the absorbed dose exceeding the threshold for deterministic effects for some organs (gonads) or tissue regions

Table 1. Equivalent organ doses and effective dose in the phantom positioned on seat 21.

Organ	**Equivalent and effective doses (mSv)**	Tissue weighting factor (ICRP 103)
Gonads[a]	1661	0.08
RBM	233	0.12
Colon	358	0.12
Lungs	104	0.12
Stomach	129	0.12
Breast[b]	-	-
Bladder	641	0.04
Liver	108	0.04
Oesophagus	67	0.04
Thyroid	63	0.04
Bone surface	201	0.01
Brain	45	0.01
Salivary glands	87	0.01
Skin	449	0.01
Remainder tissues[c]	125	0.12
Effective dose	**329**	

[a]The dose to the gonads is the dose to the testes.
[b]The dose to the breasts was not measured.
[c]Remainder tissues encompass extrathoracic region, lymphatic nodes, muscle, oral mucosa, thymus, adrenals, kidneys, pancreas, small intestine and spleen.

(figure 7) on the one hand and being comparatively small for other radiation sensitive organs on the other hand (e.g. thyroid), the effective dose is a quantity of limited usefulness.

3.3. Dose assessment using personal objects (mobile phones, chip cards)

Dose measurements using resistors of the circuit board (OSL), display screen (TL), the encapsulation of chip cards (OSL), salt dosimeters (OSL) and dental ceramics (TL/OSL) were conducted between eight and 20 d after the exposure. Full details with an in-depth analysis will be given elsewhere (Discher *et al* 2020). Here, a compilation of the main results is reported: For both exposure days with the weaker (0.65 TBq) and stronger (1.5 TBq) source a good agreement between reference dose values and measured doses in the resistor substrates and glass display for doses in excess of 50–100 mGy was observed. For chip cards, the potential as an emergency dosimeter could be demonstrated but the agreement between measured and reference doses was less satisfactory due to issues in fading correction and reference dosimetry, which requires more research work. For the TL method on display glass, outliers with a significant dose overestimation were observed in some cases, which could be identified by comparison with the results of the resistor substrates dose assessment on the same phone. Although in a real accident it could not necessarily be decided which of the two doses would then be closer to the true dose, the dose discrepancy would at least flag these samples as problematic, warranting re-investigation and the consideration of additional dose assays. There were no reference doses for the dental ceramics, but comparison with doses on the nearest personal dosimeters on the phantom indicated that the measured doses were reasonable. Salt dosimeters showed somewhat higher doses than adjacent TLDs based on LiF. For mobile phones and chip

cards, no method was (yet) able to reconstruct doses below 50 mGy with the instrumentation used, due to either insufficient sensitivity or the presence of intrinsic (confounding) signals.

3.4. Inter-laboratory comparison

For biological dosimetry, the results showed a clear decrease of measured doses with increasing distance (seat position) from the source. For OSL of mobile phones, there was a general agreement of measured doses with the results of the biological assays, however in a few cases outliers with a significant dose overestimation were found. Similar to the combination of TL of glass and OSL of resistor dose assessment within the same phone (which was not tested in the inter-comparison), the outliers could be identified by comparison with the results of biological dosimetry. Excluding the outliers, the scatter of the physical retrospective dosimetry data and average agreement with reference doses was comparable to the previous inter-comparison (Bassinet *et al* 2014). The exercise clearly demonstrated the importance of using a network-multi-parameter approach to avoid misclassifications, optimise assay robustness and time of response, and increase measurement capacity for large-scale radiological incidents. Full details are given in Woda *et al* (2020).

4. Summary and conclusions

The field test as a proof-of-concept was a unique opportunity to evaluate recently emerged dose reconstruction techniques and to inter-compare physical retrospective and biological dosimetry for the first time in a realistic accident scenario. The Cochabamba incident served as a template for the field test, mimicking an accidental eight hour exposure of passengers on an intercity bus due to an unshielded Ir-192 source in the baggage compartment. The complex and highly heterogeneous exposure geometry throughout the bus, with shielding, self-shielding effects and strong dose gradients was clearly resolved by the TLD and OSLD measurements on the various water canisters and phantoms and by the organ dose measurements in one of the phantoms. Results for the exposure with the 0.65 TBq source are somewhat higher but in a similar range as the results obtained by the IAEA in a similar dose reconstruction experiment in a response to the Cochabamba incident in (2002). The difference is ascribed to the shorter distance between source and canisters/phantoms used in the present setup. In this context, it should be emphasised once again that the aim of the field test was not to reconstruct the doses of the Cochabamba incident as close as possible but to evaluate newly developed retrospective dosimetry methods; therefore, the setup was optimised for the latter and not for the former.

Although details of the physical retrospective dosimetry technique and inter-comparison exercise results will be published in follow-up papers, it can already be summarised here that overall a good agreement between reference doses and measured doses was observed for the majority of cases. Occasional outliers occurred that could be identified by combining the results of several assays. The field test thus convincingly evaluated the potential and limitation of retrospective dosimetry using personal objects and biological dosimetry and demonstrated the importance of using a multi-parameter approach to increase robustness of the methods.

Acknowledgments

The research leading to these results has received funding from the European Commission's Seventh Framework Program (FP7/2007-2013) under grant agreement n° 261693. We are grateful to Mr. Rodolfo Suarez (IAEA) for providing electronic dosimeters and TLDs, the

Austrian Army and the entire CATO field team for fantastic on-site support and to Jérémie Dabin (SCK CEN) for carrying out the organ dose measurements and calculations for the phantom. Last but not least, we are grateful to the reviewers for their contribution to improving this publication.

References

Ademola J A, Woda C and Bortolin E 2017 Thermoluminescence investigations on tobacco dust as an emergency dosimeter *Radiat. Meas.* **106** 443–9
Ainsbury E A *et al* 2011 Review of retrospective dosimetry techniques for external ionising radiation exposures *Radiat. Prot. Dosim.* **147** 573–92
Badie C *et al* 2013 Laboratory intercomparison of gene expression assays *Radiat. Res.* **180** 138–48
Bailiff I K, Sholom S and Mckeever S W S 2016 Retrospective and emergency dosimetry in response to radiological incidents and nuclear mass-casualty events: A review *Radiat. Meas.* **94** 83–139
Bassinet C *et al* 2014 Retrospective radiation dosimetry using OSL of electronic components: results of an inter-laboratory comparison *Radiat. Meas.* **71** 475–9
Bortolin E, Boniglia C, Della Monaca S, Gargiulo R and Fattibene P 2011 Silicates collected from personal objects as a potential fortuitous dosimeter in radiological emergency *Radiat. Meas.* **46** 967–70
Cauwels V, Beerten K, Vanhavere F and Lievens L 2010 Accident dosimetry using chipcards *Proc. Third European IRPA Congress* (Helsinki, Finland) pp 866–74 (https://www.irpa2010europe.com/pdfs/proceedings/S04-P04.pdf)
Depuydt J *et al* 2017 RENEB intercomparison exercises analyzing micronuclei (Cytokinesis-block Micronucleus Assay) *Int. J. Radiat. Biol.* **93** 36–47
Discher M and Woda C 2013 Thermoluminescence of glass display from mobile phones for retrospective and accident dosimetry *Radiat. Meas.* **53–54** 12–21
Discher M, Woda C, Ekendahl D, Rojas Palma C and Steinhäusler F 2020 Evaluation of physical retrospective dosimetry methods in a realistic accident scenario: results of the CATO field test *Radiat. Meas.* (submitted)
Ekendahl D, Bulánek B and Judas L 2016 A low-cost personal dosemeter based on optically stimulated luminescence (OSL) of common household salt (NaCl) *Radiat. Meas.* **85** 93–98
Ekendahl D and Judas L 2012 Retrospective dosimetry with alumina substrate from electronic components *Radiat. Prot. Dosim.* **150** 134–41
Ekendahl D, Judas L and Sukupova L 2013 OSL and TL retrospective dosimetry with a fluorapatite glass-ceramic used for dental restorations *Radiat. Meas.* **58** 138–44
Fattibene P and Wojcik A 2009 Biodosimetric tools for a fast triage of people accidentally exposed to ionising radiation *Annali dell'Istituto Superiore di Sanità* **45** 245
Fiedler I and Woda C 2011 Thermoluminescence of chip inductors from mobile phones for retrospective and accident dosimetry *Radiat. Meas.* **46** 1862–5
IAEA - International Atomic Energy Agency 1988 The radiological accident in Goiânia STI/PUB/815 (Vienna: IAEA)
IAEA - International Atomic Energy Agency 2004 The Radiological Accident in Cochabamba STI/PUB/1199 (Vienna: IAEA)
IAEA – International Atomic Energy Agency 2002 The Radiological Accident In Gilan Sti/Pub/1123 (Vienna: IAEA)
ICRP - International Commission on Radiological Protection 2007 Recommendations of the International Commission on Radiological Protection ICRP Publication 103 *Ann. ICRP* 37 (2–4)
ICRU – International Commission on Radiation Units and Measurements 2019 Methods for initial-phase assessment of individual doses following acute exposures to ionizing radiation *ICRU Report* 92
Inrig E L, Godfrey-Smith D I and Khanna S 2008 Optically stimulated luminescence of electronic components for forensic, retrospective, and accident dosimetry *Radiat. Meas.* **43** 726–30
Jaworska A *et al* 2015 Operational guidance for radiation emergency response organisations in Europe for using biodosimetric tools developed in EU MULTIBIODOSE project *Radiat. Prot. Dosim.* **164** 165–9

Kulka U *et al* 2017 RENEB - running the European network of biological dosimetry and physical retrospective dosimetry *Int. J. Radiat. Biol.* **93** 2–14
Lee J I, Kim H, Kim J L, Pradhan A S, Kim M C, Chang I, Lee S K, Kim B H, Park C Y and Chung K S 2017 Thermoluminescence of chip inductors and resistors in new generation mobile phones for retrospective accident dosimetry *Radiat. Meas.* **105** 26–32
Oestreicher U *et al* 2017 RENEB intercomparisons applying the conventional Dicentric Chromosome Assay (DCA) *Int. J. Radiat. Biol.* **93** 20–29
Pandey D K 2016 Radioactive material removed from Delhi scrap shop (available at: www.thehindu.com/news/national/Radioactive-material-removed-from-Delhi-scrap-shop/article16365328.ece)
Pascu A, Vasiliniuc S, Zeciu-Dolha M and Timar-Gabor A 2013 The potential of luminescence signals from electronic components for accident dosimetry *Radiat. Meas.* **56** 384–8
Pradhan A S, Lee J L and Kim J L 2014 Use of OSL and TL of electronic components of portable devices for retrospective accident dosimetry *Defect Diffus. Forum* **347** 229–45
Rothkamm K *et al* 2013 Comparison of established and emerging biodosimetry assays *Radiat. Res.* **180** 111–9
Sholom S and Mckeever S W S 2014 Emergency OSL dosimetry with commonplace materials *Radiat. Meas.* **61** 33–51
Woda C, Bassinet C, Trompier F, Bortolin E, Della Monaca S and Fattibene P 2009 Radiation-induced damage analysed by luminescence methods in retrospective dosimetry and emergency response *Ann. Ist. Super. Sanita* **45** 297–306
Woda C *et al* 2020 Retrospective Dosimetry using OSL of electronic components and biological dosimetry in a realistic accident scenario: results of an inter-comparison (submitted)
Woda C and Spöttl T 2009 On the use of OSL of wire-bond chip card modules for retrospective and accident dosimetry *Radiat. Meas.* **44** 548–53
Wojcik A, Oestreicher U, Barrios L, Vral A, Terzoudi G, Ainsbury E, Rothkamm K, Trompier F and Kulka U 2017 The RENEB operational basis: complement of established biodosimetric assays *Int. J. Radiat. Biol.* **93** 15–19
World Nuclear Association 2020 Fukushima Daiichi Accident (available at: https://world-nuclear.org/information-library/safety-and-security/safety-of-plants/fukushima-daiichi-accident.aspx)